# Krylov-Projected Quantum Monte Carlo Method

N. S. Blunt,[*] Ali Alavi, and George H. Booth[†]

*University Chemical Laboratory, Lensfield Road, Cambridge CB2 1EW, United Kingdom;*
*Max Planck Institute for Solid State Research, Heisenbergstraße 1, 70569 Stuttgart, Germany;*
*and Department of Physics, King's College London, The Strand, London WC2R 2LS, United Kingdom*

We present an approach to the calculation of arbitrary spectral, thermal, and excited state properties within the full configuration interaction quzantum Monte Carlo framework. This is achieved via an unbiased projection of the Hamiltonian eigenvalue problem into a space of stochastically sampled Krylov vectors, thus, enabling the calculation of real-frequency spectral and thermal properties and avoiding explicit analytic continuation. We use this approach to calculate temperature-dependent properties and one- and two-body spectral functions for various Hubbard models, as well as isolated excited states in *ab initio* systems.

The quantum Monte Carlo (QMC) method in its various guises, is undoubtedly one of the most important approaches for accurate elucidation of properties for correlated systems [1–5]. However, these successes have focused primarily on the ground state energy and observables which commute with the Hamiltonian. Critical importance for a deeper understanding of correlated systems comes from dynamic correlation functions and spectral quantities. These mirror how we perceive our environment, namely, by perturbing a system and measuring its response—the basis of nearly all spectroscopic and experimental approaches. This gives us direct insight into optical, magnetic, and other beyond-ground-state properties, and allows for direct comparison to experimental results.

Direct access to dynamic properties is a persistent difficulty for QMC approaches in general. While, in the absence of a sign problem, unbiased imaginary-time spectra can be obtained [6–8], the analytic continuation to physical, real-frequency functions is notoriously ill conditioned and can lead to artifacts and smoothing of features [9]. For more general Fermionic systems, higher temperatures must be simulated to alleviate the sign problem [10], while nodal constraints bias towards a particular solution and are difficult to extend to spectra [1,7,11]. Alternatively, projections into effective Hamiltonians have been able to obtain a few low-energy states, but again, these are isolated states rather than practical approaches for thermal or spectral quantities [12,13], while a modification of the propagator can lead to debilitating time step issues [14].

Here, we present a new QMC approach for computing dynamic correlation functions, temperature-dependent quantities, and isolated excited states for correlated quantum systems, even in the presence of a sign problem. These correlation functions are unbiased in the limit of large averaging and exact in the limit of a large walker number. This is achieved by extending the recently developed full configuration interaction quantum Monte Carlo (FCIQMC)

method [2,15,16], by combining it with ideas from the dynamical and finite-temperature Lanczos methods (FTLM) [17–19]. The key advantage of the approach is that it avoids any explicit storage over the full Hilbert space, instead, only storing occupied states in the discretized wave function at each snapshot. This allows for sparsity in the wave function to be exploited to minimize memory bottle-necks, which are a primary limitation in conventional approaches which require explicit storage over the space [17,18,20,21]. The result is a QMC method which, although weakly exponentially scaling, in common with the ground state FCIQMC approach, can allow for systems to be treated well outside that possible by conventional means, and which retains many of the important features of the parent method [15,22,23]. These include a cancellation algorithm to ameliorate the sign problem, an absence of time-step error, and large-scale parallelism.

An arbitrary dynamic correlation function is defined as

$$G(\omega) = \langle \Psi_0 | \hat{A}^\dagger \frac{1}{\omega - (\hat{H} - E_0) + i\eta} \hat{V} | \Psi_0 \rangle, \qquad (1)$$

where $\hat{H}$ represents the Hamiltonian of the system, $\{|\Psi_0\rangle; E_0\}$ is the ground state wave function and energy, $\eta$ is a small broadening parameter, and $\hat{V}$ and $\hat{A}$ are arbitrary operators which define the perturbation and observed quantity in the correlation function. In the case of these operators being single annihilation and creation operators, one obtains the single-particle Green function, defining the system band structure and density of states.

The aim of our method is to stochastically obtain a projection of the Hamiltonian from the complete Hilbert space to an effective, reduced dimensionality space, such that it spans the degrees of freedom required to accurately describe the desired spectral or thermal quantity. In this Letter, we use a set of stochastically sampled wave functions from a FCIQMC calculation to define this transformation. If the initial state of the calculation is a

stochastic representation of the wave function $\hat{V}|\Psi_0\rangle$, then propagation from this state [24] to the ground state will, in principle, span all states required to represent the expression in Eq. (1), equivalent to the space of ground state and all imaginary-time response vectors. Once the Hamiltonian is projected into this space, it can be exactly diagonalized, and the desired correlation function of Eq. (1) directly constructed in this eigenbasis—the Lehmann representation. For thermal quantities, the approach is analogous with the initial vector taken from the infinite-temperature distribution. Similar themes have been explored within continuous real-space QMC approaches, but applied to accelerate convergence for ground state properties [25].

*Method.*—A FCIQMC iteration consists of stochastically applying a projection operator, $P$, to a walker distribution, denoted at iteration $i$ by $q_i$, such that exact projection is achieved on average, whose distributions we denote as $\psi_i$ [24]. The aim is to stochastically sample the Krylov subspace $\{\psi_0, P\psi_0, \ldots, P^{n-1}\psi_0\}$. In projector QMC approaches, one samples from the large $n$ limit of this subspace, which converges to the ground state. However, to obtain finite-temperature and dynamic quantities, the aim is now to stochastically project the Hamiltonian into the whole sampled Krylov subspace, which represents an efficient span of all states of interest, provided that $q_0$ is chosen appropriately.

By averaging the FCIQMC walker amplitudes, the results of an exact propagation are rigorously approached for expectation values which depend linearly on the wave function [15,16]. In this work, quadratic quantities are required, but now, $E[q_i^\dagger q_j] \neq \psi_i^\dagger \psi_j$, due to correlations between walker amplitudes, where $E[q_i]$ denotes the expectation value. To compute these, two independent replica sets of walkers are propagated simultaneously (indexed via superscripts), such that the amplitudes are uncorrelated between them [26,27], allowing for unbiased estimates of $\psi_i^\dagger \psi_j$ as $E[q_i^{1\dagger} q_j^2]$ or $E[q_i^{2\dagger} q_j^1]$. This approach for static correlation functions has been found to scale without difficulty within the FCIQMC approach [28] (see Supplemental Material for further details on scaling in the replica approach [29]).

At selected iterations in an FCIQMC calculation, the walker distribution is stored [30], and the overlap ($S$) and Hamiltonian ($T$) matrices between these subspace vectors are calculated as

$$S_{ij} = (q_i^{1\dagger} q_j^2 + q_i^{2\dagger} q_j^1)/2, \qquad (2)$$

$$T_{ij} = (q_i^{1\dagger} H q_j^2 + q_i^{2\dagger} H q_j^1)/2. \qquad (3)$$

While the overlap matrix estimate is trivial, calculating the $T$ matrix exactly is expensive, and so, instead, it is stochastically sampled in the same manner as spawning steps in the FCIQMC method [28]. Thus, a simulation provides an estimate of the overlap matrix and the projected Hamiltonian in the basis of Krylov vectors chosen, and so, we denote the method the Krylov projected (KP)-FCIQMC

method. Averaging these quantities over independent simulations can reduce errors in an unbiased manner, resulting in a generalized eigenvalue problem for the projected Hamiltonian. This can be solved by standard techniques (see Supplemental Material [29,31,32]). Many of the eigenvalues of $S$ will be very small (or even negative within stochastic errors), since the sampled space becomes increasingly linearly dependent with continued propagation. Therefore, we discard these vectors of $S$ without a substantial loss of information. We refer to the eigenvectors which are kept as Löwdin vectors. We note that although the estimates of $T$ and $S$ are unbiased, the final eigenvalues will not be because eigenvalues are nonlinear functions of these matrices. However, this bias can be systematically reduced with further averaging of $T$ and $S$. (see Supplemental Material for more details on the non-linear effects on the eigenvalues [29]).

For exact propagation with $\hat{P} = \hat{H}$, our approach will yield results identical to the Lanczos method. However, because the method exploits sparsity via a stochastic representation of the wave functions, large calculations can often use significantly less memory than an equivalent Lanczos calculation, as has been the case for the ground-state FCIQMC method. Although our approach is, in theory, systematically improvable to exactness for the entire frequency range, in practice, this becomes increasingly difficult for higher energy excitations. This is because high-energy excitations have a small component in the Krylov vectors, which decreases exponentially with imaginary time. This renders them particularly difficult to sample and susceptible to stochastic error in the sampled matrices. Despite this limitation, the approach can, nevertheless, be expected to obtain near-exact spectra for low-energy excitations in systems out of reach of traditional dynamical Lanczos approaches.

*Finite temperature.*—We assess the method with the half-filled Hubbard model (defined in the Supplemental Material [29]) [16,22]. Within the FTLM, thermal expectation values are computed via

$$\text{Tr}(e^{-\beta \hat{H}} \hat{A}) = \sum_{n=1}^{N} \sum_{i=0}^{M-1} e^{-\beta E_i^n} \langle n|\psi_i^n\rangle \langle \psi_i^n|\hat{A}|n\rangle + O(\beta^M),$$

$$(4)$$

where $|n\rangle$ labels a state in the $N$-dimensional Hilbert space, and $i$ labels the $M$ states of an eigensystem $\{|\psi_i^n\rangle; E_i^n\}$ resulting from a Lanczos subspace with initial state $|n\rangle$. Thus, by performing $N$ Lanczos calculations consisting of $M-1$ applications of $\hat{H}$ each, one can obtain thermal quantities which are correct to order $\beta^{M-1}$. $N$ can be very large for systems of interest, and so, in practice, one starts from a much smaller number of states, $R \ll N$, chosen as a random linear combination of all basis states, $|r\rangle = \sum_n \eta_{rn}|n\rangle$. This turns out to converge quickly with $R$, particularly at high temperatures [17,18,33–35]. In our stochastic approach, the initial random vectors are created
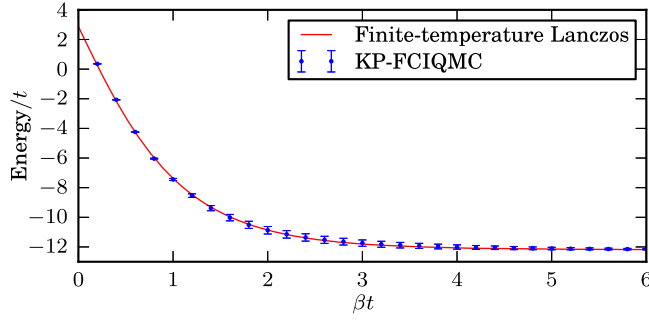
FIG. 1 (color online).　$E(\beta)$ for the 12-site 1D Hubbard model at $U/t = 1$ sampled with $\sim 2 \times 10^3$ walkers, with comparison FTLM. Error bars show standard deviation (note: not standard error) over ten independent calculations to demonstrate the spread of results. High and low temperature results are almost exact, while at intermediate temperatures, the variance in the stochastic sampling as well as systematic errors (such as from the nonlinear diagonalization step, and finite $R$) increases the variation between runs. Simulation parameters were $\tau = 0.01$, $n_a = 2.0$, and a deterministic space of double excitations [36,37].

by distributing a given number of walkers randomly throughout the Hilbert space with coefficients $\pm 1$. These initial states represent stochastic snapshots of the high-temperature limit which is exactly reproduced in the limit of large $R$.

As an initial test, Fig. 1 presents the temperature-dependent energy, $E(\beta)$, in the one-dimensional 12-site Hubbard model at $U/t = 1$. Including all symmetry sectors, the Hilbert space dimension is $\approx 3 \times 10^6$, with the largest symmetry sector containing $\approx 7 \times 10^4$ determinants. However, the system is significantly undersampled with only $2 \times 10^3$ walkers used throughout, with the projected Hamiltonian and overlap matrices averaged over ten calculations for each initial vector, $|r\rangle$. All symmetry sectors were obtained in one calculation, rather than symmetry blocking Eq. (4), resulting in a choice of $R = 1250$, while the number of Krylov vectors used was $M = 20$, with eight Löwdin vectors kept to form the final space. The results were found not to change significantly by including more Löwdin vectors.

At high temperatures, results are calculated with great accuracy. This is easily understood because the quantity calculated at $\beta = 0$, $\sum_{r=1}^{R} \sum_{i=0}^{M} \langle r|\hat{H}|\psi_i^r\rangle\langle\psi_i^r|r\rangle$, is rigorously equal to $\sum_{r=1}^{R} \langle r|\hat{H}|r\rangle$, and therefore, the quality is mainly dependent on the sampling of the initial vectors (and not on the error of individual eigenvalue estimates). At low temperatures, the results are dominated by the ground state, which has a large component in the sampled Krylov vectors and, so, is accurately calculated by the KP-FCIQMC method. However, at intermediate temperatures, the errors are larger. The most significant source of error is in replacing an exact trace over $\{|n\rangle\}$ by an approximate one over $\{|r\rangle\}$ in Eq. (4).

In Fig. 2, $E(\beta)$ for the two-dimensional 18-site Hubbard model at $U/t = 1$ is presented. Including all symmetry
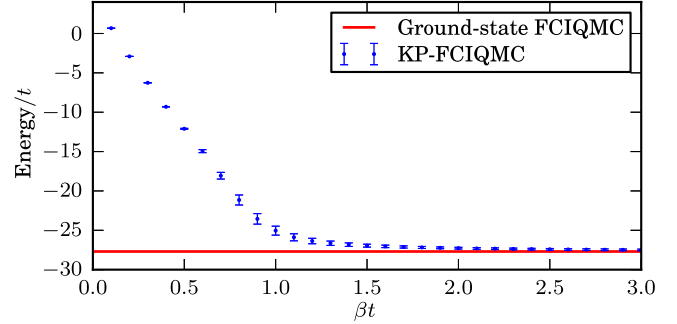


FIG. 2 (color online).　$E(\beta)$ for the 18-site 2D Hubbard model at $U/t = 1$, with ground-state FCIQMC energy for comparison. Ten independent simulations were used to create the standard deviations shown as error bars. Simulation parameters were $\tau = 0.01$, $n_a = 2.0$, and a deterministic space of double excitations.

sectors, the Hilbert space dimension is $\approx 9 \times 10^9$, with the largest symmetry sector containing $\approx 1 \times 10^8$ determinants. Again, the space was undersampled, with $5 \times 10^6$ walkers used throughout, with $R = 250$ and $M = 20$, of which 12 Löwdin vectors are kept. Since FTLM was unfeasible, also plotted is a highly accurate ground-state FCIQMC energy for comparison. A complete calculation took around $\sim 3000$ core hours. We find, again, that the high-temperature results have only a small variation between repeated calculations, and we have a high degree of confidence here. At lower temperatures, the confidence in the results is reduced, with possible systematic errors including initiator error, bias in the eigenvalue estimates, and an insufficient choice of $R$.

*Dynamical correlation functions.*—To demonstrate the ability of the KP-FCIQMC method to calculate dynamical quantities, we first consider the following zero-temperature $k$-resolved single particle Green function, defined from Eq. (1) with $\hat{V} = \hat{A} = \hat{c}_{k\downarrow}^\dagger$. The corresponding spectral function, $A_1(k, \omega) = -(1/\pi)\text{Im}[G(k, \omega)]$, defines the band structure of the material. The initial walker distribution is given by the perturbed ground state, $\hat{c}_k^\dagger|\Psi_0\rangle$, where $|\Psi_0\rangle$ is obtained from a prior ground-state FCIQMC calculation. This starting wave function ensures that, on average, the component of a particular eigenstate in any imaginary-time snapshot is proportional to its transition amplitude in the correlation function. This approach works particularly well for spectra dominated by a small number of states with large transition amplitudes. Because the transformation to the Löwdin basis introduces large errors if many states are kept (due to small overlap eigenvalues), we typically limit the number of Löwdin vectors to between 10 and 20, which limits the resolution of the spectrum. Furthermore, high-energy states die away rapidly in the Krylov vectors, and so, there tends to be significant stochastic errors associated with the calculation of such states. Although this limits the accuracy of the KP-FCIQMC method over a large energy range, we find that the method is capable of producing accurate spectra in the critical low-energy region and can accurately capture important features such as band gaps.
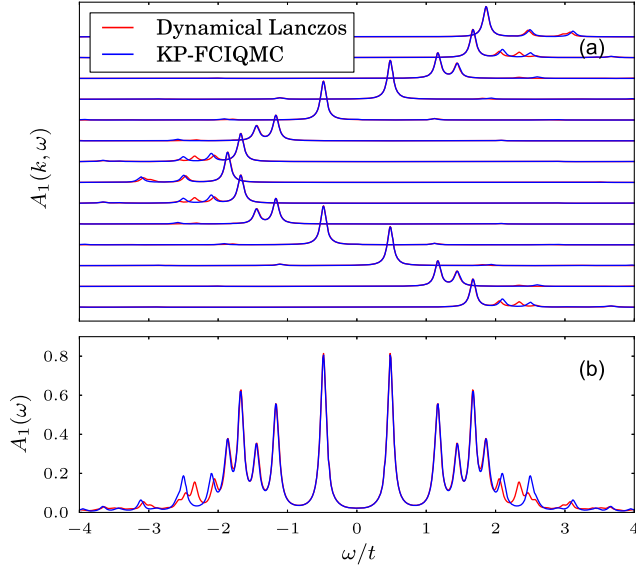
FIG. 4 (color online). $A_2(\omega)$ calculated for the 10-site Hubbard model with $U/t = 1$, and compared to the near-exact dynamical Lanczos method. Inset shows integrated weight, $\int_0^\omega A_2(\omega')d\omega'$. Simulation parameters were $\tau = 0.01$, with a deterministic space of double excitations.

FIG. 3 (color online). (a) $A_1(k,\omega)$ from $k = -\frac{6}{7}\pi$ (bottom) to $k = \pi$ (top) for the 1D 14-site Hubbard model at $U/t = 2$, compared to dynamical Lanczos method. Poles coming from the ground state or low-lying excited states with large transition amplitudes are captured accurately. (b) The local density of states. The low-energy results are reproduced accurately by the KP-FCIQMC method while the qualitative behavior is captured at high energies. Simulation parameters were $\tau = 0.01$, $n_a = 3.0$, and a deterministic space of 50 000 determinants [36].

Figure 3(a) presents $A_1(k,\omega)$ for the 14-site Hubbard model at $U/t = 2$ with $\sim 10^5$ walkers, with $S$ and $T$ averaged over ten repeats. Thirty-five Krylov vectors were sampled and ten Löwdin vectors were retained. A complete calculation for a given $k$ sector typically took only $\sim 6$ core hours. The results are compared to highly accurate dynamical Lanczos results, using 100 Lanczos vectors. Figure 3(b) presents the local density of states, computed from the results in (a) via $A(\omega) = (1/N)\sum_k A(k,\omega)$. The KP-FCIQMC results give high accuracy for low-energy features, with sum rules and causality conditions exactly fulfilled. Errors on individual poles can be estimated by repeating results. By comparing eigenvalue estimates from ten independent calculations, the band gap was estimated as $0.96456(14)t$ compared to the exact value of $0.96378t$.

We also consider the $s$-wave pair-pair dynamic correlation function, a two-body response property of significant relevance in the detection of superconducting quasiparticles.
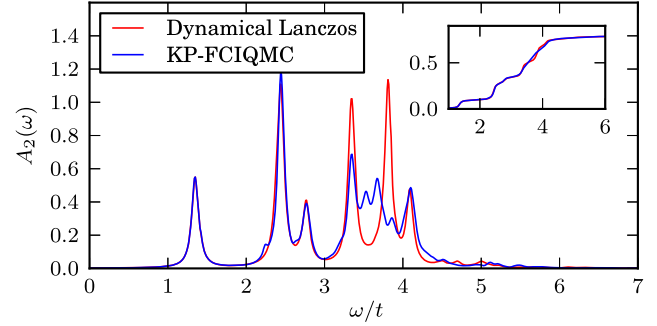
$\hat{V}$ is defined by the singlet pairing operator, $\Delta_i = (1/\sqrt{2})(c_{i\uparrow}c_{i+1,\downarrow} - c_{i\downarrow}c_{i+1,\uparrow})$, with $\hat{A} = \hat{V}$. In Fig. 4, we present results for this pairing spectrum $[A_2(\omega)]$ for the 10-site Hubbard model at $U/t = 1$, by computing all $k$-space contributions. The number of walkers was typically between $10^3$ and $10^4$. The initiator adaptation was not applied because the walker population is above the plateau [16] height for this system. No averaging of $T$ or $S$ over repeated calculations was performed. Once again, it is found that low-energy features are calculated accurately, but the quality decreases for higher energy regions of the spectrum.

*Isolated excited states.*—As a further application to larger-scale *ab initio* systems, we consider the all-electron ground and first excited state of Neon, in augmented correlation-consistent valence double zeta (aug-cc-pVDZ) and augmented correlation-consistent valence triple zeta (aug-cc-pVTZ) basis sets [38]. We work in spaces where $M_s$ is constrained to be zero, but the total spin, $S^2$, is not. The $S = 0$ and $S = 1$ states are, therefore, both contained within the same symmetry sector, and the spin gap can be directly targeted with the KP-FCIQMC method. The determinant space sizes with these two basis sets are $\sim 1.4 \times 10^8$ and $\sim 2.3 \times 10^{11}$, respectively. In order to ensure large components of the desired states in the sampled Krylov vectors, the initial wave function was created from a linear combination of trial estimates of the ground and first excited states at the inexpensive configuration interaction with singles and doubles level of theory.

TABLE I. Results for the ground ($S = 0$) and first excited ($S = 1$) states of the Ne atom ($E_h$), comparing the KP-FCIQMC method with the DMRG results (using M = 500 spin-adapted renormalized states for the larger basis) [42,43]. $\tau = 0.001$, $n_a = 3$, and a deterministic space of single and double excitations.

| Basis set | $S = 0$ | | $S = 1$ | |
| --- | --- | --- | --- | --- |
| | KP-FCIQMC | DMRG | KP-FCIQMC | DMRG |
| aug-cc-pVDZ | −128.711 43(4) | −128.711 47 | −127.977 87(5) | −127.977 94 |
| aug-cc-pVTZ | −128.825 8(1) | −128.825 14 | −128.109(1) | −128.109 19 |

KP-FCIQMC results are presented in Table I, with density matrix renormalization group (DMRG) results for comparison. The DMRG is a highly accurate algorithm, which can also be extended to thermal and spectral quantities and, so, is a suitable choice for comparison [39–41]. KP-FCIQMC results and errors were estimated by averaging over ten independent calculations. For the aug-cc-pVDZ results, $2 \times 10^5$ walkers were used, while $2 \times 10^6$ walkers were used for the aug-cc-pVTZ basis, with each calculation taking around 100 core hours for this larger basis. Calculations used 35 Krylov vectors, with ten Löwdin vectors retained, providing excellent agreement with the DMRG results.

*Conclusion.*—We have presented a novel approach to the calculation of excited state, spectral, and thermal properties within the FCIQMC framework. In this approach, the full Hamiltonian eigenvalue problem is projected into a stochastically sampled Krylov subspace, thus, allowing finite-temperature and dynamical quantities to be calculated. Since the method exploits sparsity in the sampled wave functions, the stochastic dynamic avoids storing Krylov vectors in their entirety, rendering the approach scalable to systems sizes outside the range of the Lanczos method, although, in practice, this is likely to be restricted if attempting to probe high frequency spectral features.

*nsb37@cam.ac.uk

†george.booth@kcl.ac.uk

[1] W. M. C. Foulkes, L. Mitas, R. J. Needs, and G. Rajagopal, Rev. Mod. Phys. **73**, 33 (2001).

[2] G. H. Booth, A. Grueneis, G. Kresse, and A. Alavi, Nature (London) **493**, 365 (2013).

[3] S. Sharma, T. Yanai, G. H. Booth, C. J. Umrigar, and G. K.-L. Chan, J. Chem. Phys. **140**, 104112 (2014).

[4] Y. Virgus, W. Purwanto, H. Krakauer, and S. Zhang, Phys. Rev. B **86**, 241406 (2012).

[5] S. Sorella, Y. Otsuka, and S. Yunoki, Sci. Rep. **2**, 992 (2012).

[6] S. R. White, D. J. Scalapino, R. L. Sugar, and N. E. Bickers, Phys. Rev. Lett. **63**, 1523 (1989).

[7] M. Motta, D. E. Galli, S. Moroni, and E. Vitali, J. Chem. Phys. **140**, 024107 (2014).

[8] A. W. Sandvik and J. Kurkijarvi, Phys. Rev. B **43**, 5950 (1991).

[9] M. Jarrell and J. E. Gubernatis, Phys. Rep. **269**, 133 (1996).

[10] E. Gull, P. Werner, A. Millis, and M. Troyer, Phys. Rev. B **76**, 235123 (2007).

[11] A. J. Williamson, R. Q. Hood, R. J. Needs, and G. Rajagopal, Phys. Rev. B **57**, 12140 (1998).

[12] D. M. Ceperley and B. Bernu, J. Chem. Phys. **89**, 6316 (1988).

[13] S. Ten-no, J. Chem. Phys. **138**, 164126 (2013).

[14] G. H. Booth and G. K. -L. Chan, J. Chem. Phys. **137**, 191102 (2012).

[15] G. H. Booth, A. J. W. Thom, and A. Alavi, J. Chem. Phys. **131**, 054106 (2009).

[16] J. S. Spencer, N. S. Blunt, and W. M. C. Foulkes, J. Chem. Phys. **136**, 054110 (2012).

[17] J. Jaklic and P. Prelovsek, Phys. Rev. B **49**, 5065 (1994).

[18] P. Prelovšek and J. Bonča, *Strongly Correlated Systems* (Springer, Berlin, 2013), pp. 1–30.

[19] P. E. Dargel, A. Wollert, A. Honecker, I. P. McCulloch, U. Schollwoeck, and T. Pruschke, Phys. Rev. B **85**, 205119 (2012).

[20] A. Hams and H. De Raedt, Phys. Rev. E **62**, 4365 (2000).

[21] S. Sugiura and A. Shimizu, Phys. Rev. Lett. **111**, 010401 (2013).

[22] J. J. Shepherd, G. E. Scuseria, and J. S. Spencer, Phys. Rev. B **90**, 155130 (2014).

[23] D. Cleland, G. H. Booth, and A. Alavi, J. Chem. Phys. **132**, 041103 (2010).

[24] In FCIQMC, the propagator $\hat{P} = \mathbb{1} - \tau(\hat{H} - S\mathbb{1})$ is used, where $\tau$ is a small time step and $S$ is allowed to vary based on the walker population, $\sum_i |q_i|$, where $q_i$ is the walker weight on site $i$. See Ref. [15] for more details.

[25] M. Caffarel, F. X. Gadea, and D. M. Ceperley, Europhys. Lett. **16**, 249 (1991).

[26] S. Zhang and M. H. Kalos, J. Stat. Phys. **70**, 515 (1993).

[27] N. S. Blunt, T. W. Rogers, J. S. Spencer, and W. M. C. Foulkes, Phys. Rev. B **89**, 245124 (2014).

[28] C. Overy, G. H. Booth, N. S. Blunt, J. J. Shepherd, D. Cleland, and A. Alavi, J. Chem. Phys. **141**, 244117 (2014).

[29] See Supplemental Material at http://link.aps.org/supplemental/10.1103/PhysRevLett.115.050603 for details of the Hubbard model, the diagonalization and associated biases of the Krylov basis, and description of the scaling of the replica sampling approach.

[30] In practice, we sample the wave function with a linearly increasing number of iterations between selections, such that vectors during early iterations are sampled with finer resolution, where the wave function is rapidly changing and contains significant projections onto excited eigenstates.

[31] Z. Bai, J. Demmel, J. Dongarra, A. Ruhe, and H. van der Vorst, *Templates for the Solution of Eigenvalue Problems: A Practical Guide* (SIAM, Philadelphia, 2000).

[32] J. Cullum and R. Willoughby, *Lanczos Algorithms for Large Symmetric Eigenvalue Computations* (Birkhäuser, Boston, 1985), Vol. 2.

[33] T. Iitaka and T. Ebisuzaki, Phys. Rev. E **69**, 057701 (2004).

[34] J. Schnack and O. Wendland, Eur. Phys. J. B **78**, 535 (2010).

[35] O. Hanebaum and J. Schnack, Eur. Phys. J. B **87**, 194 (2014).

[36] F. R. Petruzielo, A. A. Holmes, H. J. Changlani, M. P. Nightingale, and C. J. Umrigar, Phys. Rev. Lett. **109**, 230201 (2012).

[37] D. M. Cleland, G. H. Booth, and A. Alavi, J. Chem. Phys. **134**, 024112 (2011).

[38] T. Dunning, J. Chem. Phys. **90**, 1007 (1989).

[39] S. R. White, Phys. Rev. Lett. **69**, 2863 (1992).

[40] S. R. White and A. E. Feiguin, Phys. Rev. Lett. **93**, 076401 (2004).

[41] A. E. Feiguin and S. R. White, Phys. Rev. B **72**, 220401(R) (2005).

[42] R. Olivares-Amaya, W. Hu, N. Nakatani, S. Sharma, J. Yang, and G. K.-L. Chan, J. Chem. Phys. **142**, 034102 (2015).

[43] S. Sharma and G. K.-L. Chan, J. Chem. Phys. **136**, 124121 (2012).